

Analytical Methods

Accepted Manuscript



This is an *Accepted Manuscript*, which has been through the Royal Society of Chemistry peer review process and has been accepted for publication.

Accepted Manuscripts are published online shortly after acceptance, before technical editing, formatting and proof reading. Using this free service, authors can make their results available to the community, in citable form, before we publish the edited article. We will replace this *Accepted Manuscript* with the edited and formatted *Advance Article* as soon as it is available.

You can find more information about *Accepted Manuscripts* in the [Information for Authors](#).

Please note that technical editing may introduce minor changes to the text and/or graphics, which may alter content. The journal's standard [Terms & Conditions](#) and the [Ethical guidelines](#) still apply. In no event shall the Royal Society of Chemistry be held responsible for any errors or omissions in this *Accepted Manuscript* or any consequences arising from the use of any information it contains.

Shell-like Sm-doped CeO₂ nanostructure based electrochemical DNA biosensor for breast cancer gene sequence detection

Cite this: DOI: 10.1039/x0xx00000x

Received 00th January 2012,

Accepted 00th January 2012

DOI: 10.1039/x0xx00000x

www.rsc.org/

Fen-fang Deng^a, Cong Ding^a, Yu Wang^{b,*}, Wen-ting Li^a, Li-li Liu^a, He Li^{a,*}

Samarium doped cerium dioxide (CSO) nanostructures possessing shell-like morphology had been synthesised by simple hydrothermal method. A novel nanocomposite membrane, comprising of CSO nanostructures, chitosan (CH) and room temperature ionic liquid (RTIL) was deposited onto an indium-tin oxide (ITO) electrode for developing a DNA biosensor related to the breast cancer gene. The properties of the CSO and nano-composite membrane were studied by thermogravimetry (TG), X-ray diffraction (XRD), energy dispersive spectrum (EDS), scanning electron microscopy (SEM), cyclic voltammetry (CV) and electrochemical impedance spectroscopy (EIS). The hybridization capacity of the DNA biosensor was studied with differential pulse voltammetric (DPV) using [Fe(CN)₆]^{3-/4-} as an indicator. Under optimal conditions, the fabricated DNA biosensor could quantify wide range of the target DNA concentration over the range of 1×10⁻¹³-1×10⁻⁶M with good linearity (R=0.9981) and a low detection limit of 1.56×10⁻¹⁴ M (3σ). Results showed that the fabricated shell-like CSO nanostructures and RTIL could enhance the electrical conductivity synergistically, which has great potential application in sensitive electrochemical biosensor.

Introduction

Breast cancer is one of the most common female malignant tumors. The BRCA1 gene encodes the tumor suppressor protein breast cancer and is linked to hereditary breast and ovarian cancer, which has a significant role in the signalling of DNA damage and in DNA repair. BRCA1 mutation carriers amount to approximately 10% of ovarian and 7% of breast cancer cases.^{1,2} Therefore, the detection and analysis of BRCA1 gene is of great significance. The conventional methods including real-time quantitative polymerase chain reaction,³ next-generation sequencing,^{4,5} enzymatic,⁶ direct probe/target hybridization,⁷ melting curve analyses,⁸ fluorescent⁹ might not be the best methods for the routine detection of BRCA1 mutations because they are relatively low sensitivity, time consuming and high cost. However, DNA electrochemical biosensors possess simplicity, high sensitivity, low cost, cheap instrument.^{10,11}

Cerium oxide (CeO₂) has attracted significant interest in the present frontier research due to its unusual properties including strong adsorption ability (high isoelectric point~9.2), large surface area, excellent biocompatibility, high chemical stability and nontoxicity.¹²⁻¹⁵ When CeO₂ is doped with impure elements, its physicochemical and electrical properties can be improved due to the exchange of oxygen in the oxide network by decreasing the energy barrier for oxygen migration.¹⁶ At high oxygen partial pressures, these CeO₂-based oxides show high oxide ionic conductivity.¹⁷

Room temperature ionic liquid (RTIL), composed of organic cations and various anions exhibits many unique advantages such as wide electrochemical windows, high ionic conductivity, high chemical and thermal stabilities, ability to dissolve different organic compounds, and ionic nature which makes them highly polar solvents.¹⁸⁻²⁰ Therefore, it is widely used in organic synthesis,²¹ catalytic chemistry,^{22,23} electrochemistry^{24,25} and other fields.

In this work, shell-like Sm-doped cerium dioxide (CSO) nanostructures were synthesized by simple hydrothermal technique and were utilized as the modified electrode by combining with RTIL and chitosan (CH). Single stranded DNA (ssDNA) related to breast cancer was adsorbed on the modified electrode to obtain a novel electrochemical DNA biosensor.

Experimental

Reagents and materials

Cerium(III) nitrate hexahydrate, samarium(III) nitrate hexahydrate, polyvinylpyrrolidone (PVP), ionic liquid 1-ethyl-3-methylimidazole four fluorine boronic acid salt ([Emim]BF₄), chitosan, sodium oxalate and other chemicals were purchased from Aladdin Reagent Company (Shanghai, China). Indium-tin-oxide (ITO) coated glass plates have been obtained from Zhuhai Kaiva Electronic Components Co., Ltd. All the probes and target oligonucleotides were synthesized by Invitrogen (Shanghai, China). The oligonucleotides were purified via polyacrylamide gel

electrophoresis (PAGE). The sequences of probes and target oligonucleotides used for DNA detection were showed in table 1.

Table 1 Oligonucleotides sequence used in this study

Probe DNA (S1)	5'-ATGTATGAATTATAATCAAAGAAACC-3'
Target DNA (S2)	5'-GGTTTCTTTGATTATAATTCATACAT-3'
One-base-mismatch(S3)	5'-GGTTTCTT <u>A</u> GATTATAATTCATACAT-3'
Two-base-mismatch(S4)	5'-GGTT <u>G</u> CTTTGATTAT <u>G</u> ATTCATACAT-3'
Non-complementary(S5)	5'-CTTCTGGTAGTCGGAGCTGATGGGG-3'

The buffer solutions were as follows: the DNA immobilization buffer containing 1×10^{-2} M Tris-HCl and 1.0×10^{-3} M EDTA (pH 8.0); the buffer for electrochemical measurements containing 1×10^{-2} M phosphate buffer solution (PBS, pH 7.0), 5 mM $[\text{Fe}(\text{CN})_6]^{3-/4-}$ solution and 0.1 M KCl; and the washing buffer containing 100 mM phosphate buffer solution (PBS, pH 7.4, 25 °C) and 0.1 M KCl.

Apparatus

Electrochemical measurements were recorded using an Autolab Potentiostat/Galvanostat (Metrohm). A conventional three-electrode cell with an Ag/AgCl reference, a platinum wire counter and the modified ITO as the working electrodes were used. Scanning electron micrograph (SEM) was obtained on Zeiss Ultra55 field emission scanning electron microscope (Carl Zeiss, Germany). X-ray diffraction (XRD) was performed with Bruker D8 advance (Bruker, Germany).

Synthesis of CSO nanostructures

The CSO nanostructures were synthesized by hydrothermal method by consulting the literature.²⁶ The hydrothermal reactions were carried out in a stainless steel autoclave with a teflon liner (100 mL in total capacity) under autogenous pressure. In a typical synthesis, 6 mmol $\text{Na}_2\text{C}_2\text{O}_4$ dissolved in 30 mL deionized water was added dropwise into 4 mmol nitrate solution (a certain proportion of $\text{Ce}(\text{NO}_3)_3$ and $\text{Sm}(\text{NO}_3)_3$) under stirring. After the addition of $\text{Na}_2\text{C}_2\text{O}_4$ solution, a white precipitate appeared and then continues stirring for 2 h. Subsequently, a specified amount of PVP was introduced into this solution with constant stirring for 2 h to form an orange suspension. Then the mixture was transformed into Teflon-lined autoclave, and heated at 180 °C for 8 h. Then cooling to room temperature naturally, the white precipitate was collected, washed with distilled water and absolute ethanol before drying in air at 60 °C for 4 h. Eventually, the as-synthesized precursors were calcined in air at a certain temperature for 4 h to obtain CSO nanostructures.

Preparation of the electrode

Prior to modification, the ITO substrates were soaked in an ultrasonic bath successively with acetone, absolute alcohol and distilled water for 5 min each time, and then dried at room temperature.

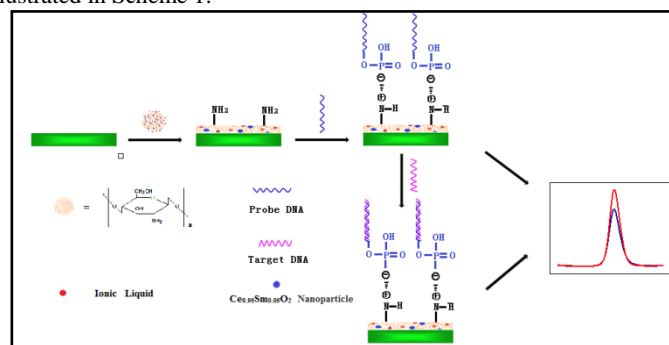
The nanocomposite solution was prepared as follows: 50 mg of CH was dissolved into 10 mL of 1% (vol.%) acetic acid solution to form a transparent CH solution; Then, a certain amount of CSO powder was dispersed into above solution and sonicated for 2h to obtain a uniform faint yellow gel of CH-CSO; Subsequently, 150 μL RTIL was added into the yellow gel with continued ultrasonication for 2 h to obtain a highly homogeneous, stable nanocomposite of CH-CSO-IL; Finally, 10 μL of above nanocomposite was pipetted onto the

surface of the cleaned ITO electrode and dried at room temperature to get a modified electrode denoted as CH-CSO-IL/ITO.

Probe DNA immobilization and hybridization

Immobilization of ssDNA probes was performed by pipetting 10 μL of 1.0 μM probe DNA (S1) on the CH-CSO-IL/ITO surface for dryness at room temperature, followed by washing with the washing buffer and ultrapure water to remove the un-immobilized ssDNA; the obtained electrode was denoted as S1/CH-CSO-IL/ITO.

For the hybridization process, the S1/CH-CSO-IL/ITO electrode was immersed in hybridization solution that contained the desired concentration of complementary (S2), 1-base mismatched (S3), 2-base mismatched (S4), and non-complementary (S5) target DNA for 70min at 45 °C. The electrodes were subsequently washed with the washing buffer and ultrapure water to remove the un-hybridized DNA as well. The hybridized electrode was denoted as S2-S1/CH-CSO-IL/ITO, S3-S1/CH-CSO-IL/ITO, S4-S1/CH-CSO-IL/ITO, S5-S1/CH-CSO-IL/ITO, respectively. The detailed fabrication and detection procedures for the developed DNA biosensor are illustrated in Scheme 1.²⁷



Scheme 1 Schematic representation of the steps for fabrication of DNA bioelectrode

Electrochemical measurements

Electrochemical measurements were investigated by cyclic voltammetry (CV), differential pulse voltammetry (DPV) and electrochemical impedance spectroscopy (EIS). The CV scans were performed at 10mV/s from -0.4 to 0.8V (vs. Ag/AgCl). EIS measurements were conducted at 0.18V over a 10-2-105 Hz frequency range, with 0.01V signal amplitude. DPV currents were obtained over a potential range from -0.15 to 0.55V with a 0.025V pulse amplitude.

Results and discussion

Synthesis conditions and characterization of CSO

Thermogravimetric analysis. As can be noted from Fig. 1, the CSO precursors exhibited one minor and one major weight loss peaks. The minor low-temperature peak in the range 80-165 °C was primarily due to the loss of nondissociative adsorbed water as well as water hold on the surface by hydrogen bonding. A further loss of water occurred around 295-452 °C due to dehydroxylation of the surface. The loss of weight from ambient to 295 °C was about 10% and from 295 to 452 °C was 30%. No further weight loss or gain was found in the temperature range of 452-800 °C. Thus over the temperature range between 452 and 800 °C, the CSO was quite stable in terms of chemical composition.

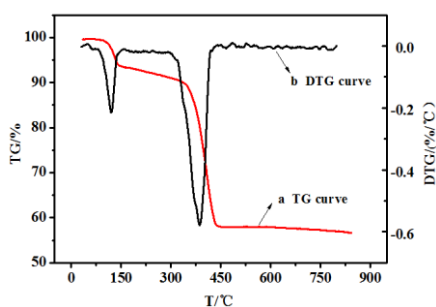


Fig. 1. TG and DTG curves show the decomposition of precursor for the preparation of CSO in air.

Optimizing the annealed temperature. Fig. 2A showed XRD patterns of CSO annealed at different temperatures from 500 to 800 °C at intervals of 100 °C. The diffraction peaks correspond to the (111), (200), (220), (311), (222), (400), (311), and (420) planes, which could be indexed as a pure cubic fluorite CeO_2 structure, and coincided well with the standard data of CeO_2 (JCPDS No. 65-2975). No obvious peaks corresponding to samarium oxide or other cerium oxides were observed in the powder pattern. We suggested the Sm was doped into crystallographic structure. Figure 2A revealed the diffraction peaks increased in intensity and decreased in width with increase of the annealing temperature due to improvement of crystallization and increase of the nanocrystalline size. According to the DPV results showed in Fig. 2B., we found that the smaller the size of CSO was, the better its electrical conductivity was. Therefore, we chose 500 °C as the best calcination temperature.

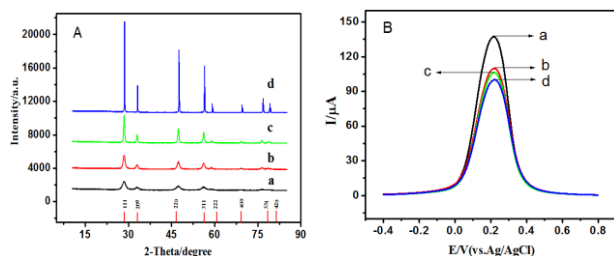


Fig. 2. XRD patterns (A) and DPV curves (B) of precursors annealed in 500 °C (a); 600 °C (b); 700 °C (c); 800 °C (d).

Optimizing the doping ratio. The doping ratio of Sm will also affect the conductivity of CSO. Therefore, we synthesized different proportion of Sm doped CeO_2 powder by hydrothermal method and calcined at 500 °C. The differential pulse voltammetry was used to investigate the different powder (Supplementary data Fig. 1). The results showed that, the peak current of un-doped CeO_2 was much smaller than that doped with 5%. When doped with 5%, the highest DPV current signal was determined. Beyond 5%, the current signal seemed to decrease gradually. Thus, the optimal doping ratio was 5%.

EDS analysis. The composition of the synthesized product was further confirmed from EDS analysis. The EDS pattern of the nanostructures is presented in the supplementary data Fig. 2. The strong peaks for Ce and Sm were found in the spectra, thus the existence of Sm was confirmed. Combining the XRD data, we could make sure the Sm had successfully doped into the lattice of CeO_2 . The unexpected but physically present element C was detected due to conducting resin. The atomic percentage of 5%

doped CSO was listed in the Supplementary data Table 1. Thus from elemental analyses, atomic percentage of Ce and Sm is 16.63:0.83, that closed to the synthesis proportion of 0.95:0.05.

SEM studies of the modified electrodes

The surface morphologies of the electrodes were examined with SEM as shown in Fig. 3. The rough and uniform morphology was observed for CH film in Fig. 3A. After adding CSO, we could see that the CSO nanostructures were well scattered on the surface of CH film with an average size of about 1 μm (Fig. 3B). From the enlarged drawing, the CSO displayed a shell-like structure morphology, which seems to be consisting of uneven in length nanorods having average diameter of about 100 nm. Meanwhile, the morphology of CH-CSO-RTIL compound displayed a porous membrane with an average diameter of about 40 μm (Fig. 3C). Fig. 3(D) showed the SEM image of the surface of bioelectrode (ssDNA/CH-CSO-IL/ITO) prepared after immobilization of DNA and it could be seen from Fig. 3D that the large morphologies of CH-CSO-RTIL matrix had been buried under layer of immobilized DNA and was attributed to very high loading of the probe DNA molecules on the electrode surface.

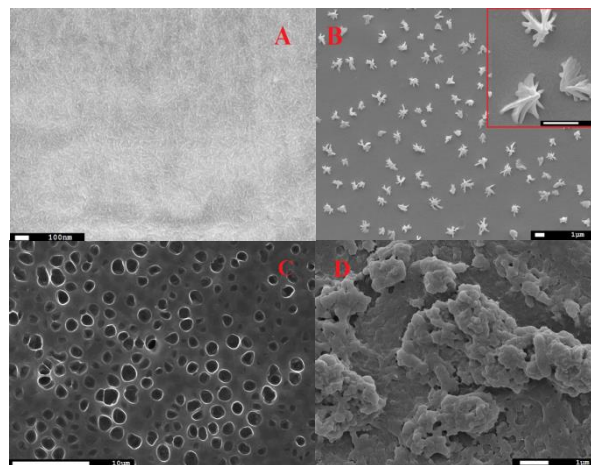


Fig. 3. SEM image of the synthesized CH/ITO electrode (A), CH-CSO/ITO electrode (B), CH-CSO-IL/ITO electrode (C) and ssDNA/CH-CSO-IL/ITO bioelectrode (D)

Electrochemical characteristics of the modified electrodes

As can be seen from Fig. 4A, the CV curve of the CH/ITO (curve a) exhibited electrochemical characteristics with a couple of redox peaks for the $[\text{Fe}(\text{CN})_6]^{3-/4-}$ mediator. The peak current of the CH-CSO/ITO (curve b) had larger CV current than CH/ITO, which ascribed to the fact that the shell-like CSO nanostructured matrix has an excellent electron transfer property and provides a large surface area for the diffusion of $[\text{Fe}(\text{CN})_6]^{3-/4-}$ towards the electrode surface. The peak current of the CH-RTIL/ITO (curve c) was also increased in comparison to that of CH/ITO, suggesting that RTIL could significantly enhance conductivity. When the CSO and RTIL were added simultaneously, the peak current of the CH-CSO-

RTIL/ITO (curve d) achieved maximum, indicating the synergistic effect of CSO and RTIL.

Electrochemical impedance spectroscopy (EIS) was employed to study the interfacial electron-transfer resistance (R_{et}) at the DNA modified electrodes. In EIS spectrum, the semicircle portion observed at high frequency in the Nyquist diagrams corresponds to the electron transfer limiting process. As illustrated in Fig. 4B It was observed that the R_{et} of the ssDNA/CH-CSO-RTIL/ITO (curve a) was significantly larger than the CH-CSO-RTIL/ITO (curve a), which could be attributed to the electrostatic repulsion between the negatively charged backbone of probe ssDNA and $[Fe(CN)_6]^{3-/4-}$ anion, confirming the effective immobilization of probe DNA. After hybridization of probe with its complementary target DNA, a further increase in R_{et} value is observed (curve c). The increase in R_{et} is expected due to increased repellence of negatively charged redox species present in the electrolyte by more negatively charged phosphate groups present on the backbone of double stranded DNA thus hindering the electron exchange process. The observation also indicates the successful hybridization of complementary probe DNA on the surface of ssDNA/CH-CSO-RTIL/ITO.

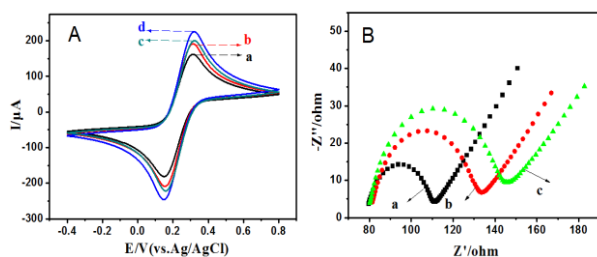


Fig. 4. (A) CV curves of (a) CH/ITO, (b) CH-CSO/ITO, (c) CH-RTIL/ITO, (d) CH-CSO-RTIL/ITO electrode; (B) EIS curves of (a) CH-CSO-RTIL/ITO, (b) ssDNA/CH-CSO-RTIL/ITO, (c) dsDNA/CH-CSO-RTIL/ITO

Fig. 5 showed cyclic voltammograms of ssDNA/CH-CSO-RTIL/ITO bioelectrode as a function of scan rate varying from 10 to $100\text{mV}\cdot\text{s}^{-1}$ in PBS (100 mM, pH 7.0) containing 5 mM $[Fe(CN)_6]^{3-/4-}$. It was observed that both cathodic (I_{pc}) and anodic (I_{pa}) peak currents of the electrode increased linearly and were proportional to the square root of scan rate (inset, Fig.5B) according to the following equations:

$$I_{pa}(\mu A) = 58.9v^{1/2} + 154.9 \quad (R^2 = 0.9899) \quad (1)$$

$$I_{pc}(\mu A) = -60.9v^{1/2} - 145.2 \quad (R^2 = 0.9913) \quad (2)$$

Where, I_{pa} was the oxidation peak current; I_{pc} was the reduction peak current; R was the relative standard deviation.

These results suggest a surface-controlled electrochemical process and reversible electron transfer in the CH-CSO-RTIL nanocomposite film.

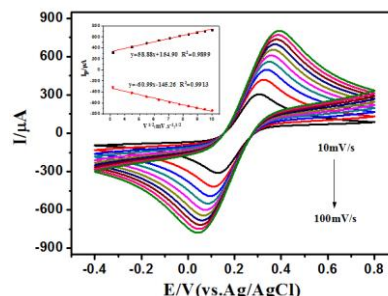


Fig. 5. CV curves of ssDNA/CH-CSO-RTIL/ITO bioelectrode at different scan rate.

Optimizing the conditions for fabricating the DNA biosensor

In order to provide the biosensor with a good performance, some parameters including the pH of the working buffer, the hybridization temperature and hybridization time were optimized.

The influence of the pH of the working buffer had been studied from 6.0 to 8.0 in PBS (100mM) containing 5mM $[Fe(CN)_6]^{3-/4-}$ using DPV. As seen in Fig.6A, the current response arrives at a maximum value at $\text{pH}=7.0$, indicating that the ssDNA/CH-CSO-IL/ITO bioelectrode has the highest bioactivity at the $\text{pH}=7.0$. Thus, the optimal $\text{pH}=7.0$ of the working buffer was chosen in the further studies.

The effect of the hybridization temperature on the response signal was investigated from 25 to 65°C . Fig. 6B illustrated that the change of peak current response, ΔI ($\Delta I = I_{\text{before}} - I_{\text{after}}$), before and after the probe DNA reaction with the target DNA, increased with temperature up to 45°C , then decreased. This is due to the fact that high temperature is contributed to accelerate the movement of biological molecules, but a certain extent temperature higher than the melting temperature speed the denaturation of dsDNA.²⁸ As a result, hybridization temperature of 45°C was selected in the subsequent work.

The hybridization time was also optimized. The result showed in Fig. 6C that the change of DPV peak current (ΔI) increased with the increase of hybridization time within the first 70 min and then leveled. The saturated hybridization indicated that the CH-CSO-RTIL film assembled on the ITO were stable. Thus, A 70 min hybridization time was used in the experiments.

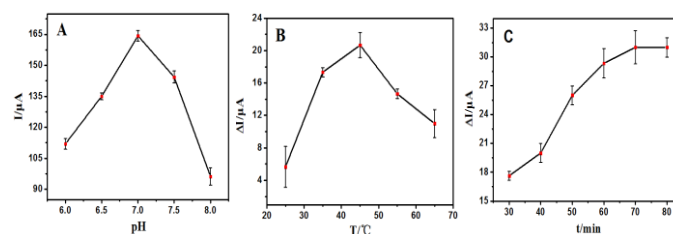


Fig. 6. (A) Differential pulse voltammetry of ssDNA/CH-CSO-RTIL/ITO electrode as a function of pH (6.0-8.0); (B) DPV response as a function of hybridization temperature (25- 65°C); (C) DPV response as a function of hybridization time (30-80min)

The DPV response and calibration curve of the DNA biosensor

Under optimal conditions, the sensitivity of the DNA biosensor was studied by using the probe DNA of $1 \times 10^{-6} \text{ M}$ to hybridize with various concentrations of the target DNA. With an increase of the target DNA concentration, the change of DPV peak current (ΔI) gradually decreased. The peak current values were linear with the logarithmic value of target DNA sequences in the range of 1.0×10^{-13} to $1.0 \times 10^{-6} \text{ M}$ (Fig. 7B). The linear regression equation was as follows:

$$\Delta I(\mu\text{A}) = 3.0832 \log(C/\text{M}) + 48.4571 \quad R^2 = 0.9981 \quad (3)$$

Where, ΔI was the change of peak current response, ($\Delta I = I_{\text{before}} - I_{\text{after}}$), before and after the probe DNA reaction with the target DNA; C was the concentration of target DNA; R was the relative standard deviation.

A detection limit of the breast cancer gene sequence was determined to be $1.56 \times 10^{-14} \text{ M}$ (3σ) (where σ is the relative standard deviation of the blank solution, $n=11$), suggesting that the proposed DNA biosensor is good enough for the breast cancer gene sequence detection.

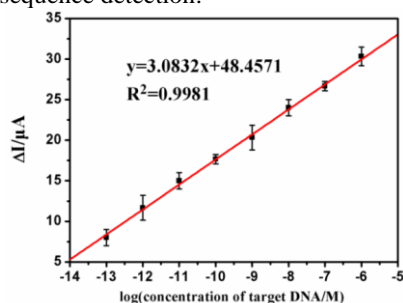


Fig. 7. The calibration plots of peak current change versus the logarithm of various concentrations of the target DNA under optimal conditions.

Selectivity, regeneration and stability of DNA biosensor

The selectivity of the sensor was investigated by measuring the changes of EIS responses (ΔR_{et} , $\Delta R_{\text{et}} = R_{\text{et, before}} - R_{\text{et, after}}$) before and after the probe DNA reaction with different kinds of target DNA sequences. The results were showed in Fig.8. It could be seen that after probe DNA hybridization with noncomplementary DNA, the ΔR_{et} value is small (a) but increased obviously after hybridization with target DNA (Curve d). After the DNA probe was hybridized with the single-base mismatched sequence (c) or double-base mismatched sequence (b), the increase of the ΔR_{et} value was much smaller than that obtained from the hybridization with target DNA (d). And the single-base mismatched sequence and double-base mismatched sequence could also be recognized via comparing the increase of the R_{et} value. The results show that the biosensor has good selectivity for hybridization detection.

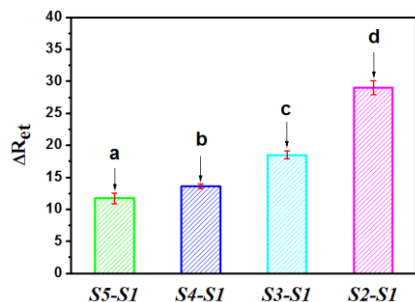


Fig. 8. The histogram of ΔR_{et} singals on S5-S1/CH-CSO-RTIL/ITO(a), S4-S1/ CH-CSO-RTIL /ITO(b), S3-S1/ CH-CSO-RTIL /ITO(c), S2-S1/ CH-CSO-RTIL /ITO(d), the concentration of the different DNA sequences was $1 \times 10^{-6} \text{ M}$.

The regeneration ability of ssDNA/CH-CSO-IL/ITO electrode has been studied by dipping the electrode in PBS of pH=7.0 hot water (80°C) for 10 min, followed by a rapid cooling in an ice bath for 10 min, then examined via DPV after its hybridization with complementary target DNA. It was found that the modified electrode could be regenerated 3 times with about 10% loss of the original signal, showing the high regeneration ability of this DNA electrochemical biosensor.

At the same time, the stability of the modified electrode was also evaluated. The modified electrode was firstly stored in the refrigerator at 4°C over 2 weeks and then examined via DPV after its hybridization with complementary target DNA. Experiments demonstrated that 90% of the initial response remained, indicating good stability.

Conclusions

In this paper, a sensitive DNA electrochemical biosensor based on a novel nanocomposite CH-CSO-RTIL was fabricated and first applied to the detection of breast cancer gene. The shell-like CSO nanostructures could greatly enhance the immobilization of the DNA probes and synergistic improve the electrical conductivity with the RTIL. The dynamic concentration range, low detection limit, high sensitivity, good stability and fine selectivity are the main features of the proposed DNA biosensor. In summary, nanocomposite CH-CSO-RTIL based bioelectrode provides an excellent sensing platform for efficient detection of DNA.

Acknowledgements

This work was supported by the Science and Technology Planning Project of Guangzhou (No.2009Z2-D511), and the Natural Science Foundation of Guangdong Province (No. 10151063101000011 and S2011040003162), China.

Notes and references

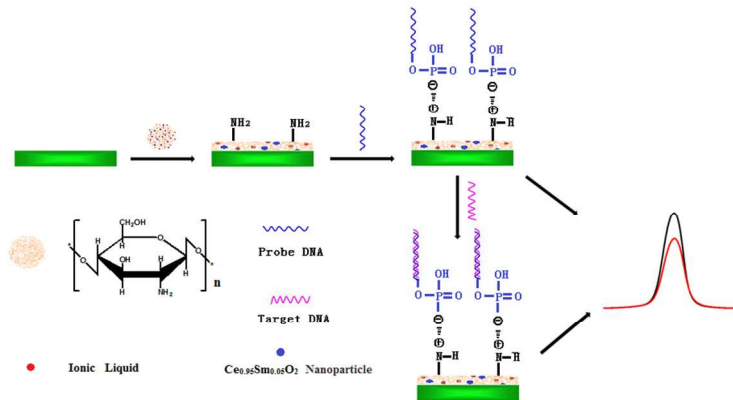
- ^a School of Chemistry and Environment, South China Normal University, Guangzhou, Guangdong 510006, P. R. China. Fax: +86-20-39310187. E-mail: analchemlh@163.com (He Li)
- ^b Department of Pathology, Zhujiang Hospital, Southern Medical University, Guangzhou 510282, P. R. China. E-mail: doctorwylh@163.com (Yu Wang)

Electronic Supplementary Information (ESI) available: [details of any supplementary information available should be included here]. See DOI: 10.1039/b000000x/

- C. Kroupis, K. Christopoulos, M. Devetzoglou, I. Tsiagas and E. S. Lianidou, *Clinica Chimica Acta*, 2008, 390, 141-144.
- E. Mavrogianopoulou, P. S. Petrou, S. E. Kakabakos and K. Misiakos, *Biosensors & bioelectronics*, 2009, 24, 1341-1347.
- C. Kroupis, A. Stathopoulou, E. Zygalki, L. Ferekidou, M. Talieri and E. S. Lianidou, *Clin. Biochem.*, 2005, 38, 50-57.

- 1 4. I. Hernan, E. Borrás, M. de Sousa Dias, M. J. Gamundi, B. Mane, G.
2 Llorca, J. A. Agundez, M. Blanca and M. Carballo, *The Journal*
3 *of molecular diagnostics : JMD*, 2012, 14, 286-293.
- 4 5. L. Y. Zhang, T. Kirchhoff, C. J. Yee and K. Offit, *J. Mol. Diagn.*,
5 2009, 11, 176-181.
- 6 6. J. Huang, X. Su and Z. Li, *Sensors and Actuators B: Chemical*, 2014,
7 200, 117-122.
- 8 7. S. C. Yim, H. G. Park, H. N. Chang and D. Y. Cho, *Analytical*
9 *biochemistry*, 2005, 337, 332-337.
- 10 8. G. Pals, K. Pindolia and M. J. Worsham, *Mol. Diagn.*, 1999, 4, 241-
11 246.
- 12 9. C. R. Twist, M. K. Winson, J. J. Rowland and D. B. Kell, *Analytical*
13 *biochemistry*, 2004, 327, 35-44.
- 14 10. J. Yang, X. Wang and H. Shi, *Sensors and Actuators B: Chemical*,
15 2012, 162, 178-183.
- 16 11. Y. L. Zhang, Y. Wang, H. B. Wang, J. H. Jiang, G. L. Shen, R. Q. Yu
17 and J. H. Li, *Anal. Chem.*, 2009, 81, 1982-1987.
- 18 12. W. Zhang, T. Yang, X. Zhuang, Z. Guo and K. Jiao, *Biosensors &*
19 *bioelectronics*, 2009, 24, 2417-2422.
- 20 13. N. Sutradhar, A. Sinhamahapatra, S. Pahari, M. Jayachandran, B.
21 Subramanian, H. C. Bajaj and A. B. Panda, *The Journal of*
22 *Physical Chemistry C*, 2011, 115, 7628-7637.
- 23 14. X. Jiao, H. Song, H. Zhao, W. Bai, L. Zhang and Y. Lv, *Analytical*
24 *Methods*, 2012, 4, 3261.
- 25 15. S. Kundu, N. Sutradhar, R. Thangamuthu, B. Subramanian, A. B.
26 Panda and M. Jayachandran, *J. Nanopart. Res.*, 2012, 14.
- 27 16. A. B. Kehoe, D. O. Scanlon and G. W. Watson, *Chemistry of*
28 *Materials*, 2011, 23, 4464-4468.
- 29 17. T. Mori, J. Drennan, J. H. Lee, J. G. Li and T. Ikegami, *Solid State*
30 *Ion.*, 2002, 154, 461-466.
- 31 18. F. Zhao, X. Wu, M. K. Wang, Y. Liu, L. X. Gao and S. J. Dong, *Anal.*
32 *Chem.*, 2004, 76, 4960-4967.
- 33 19. C.-H. Liu, B.-H. Mao, J. Gao, S. Zhang, X. Gao, Z. Liu, S.-T. Lee,
34 X.-H. Sun and S.-D. Wang, *Carbon*, 2012, 50, 3008-3014.
- 35 20. F. Lu, X. Ji, Y. Yang, W. Deng and C. E. Banks, *RSC Advances*,
36 2013, 3, 18791.
- 37 21. T. Alammari and A.-V. Mudring, *Materials Letters*, 2009, 63, 732-
38 735.
- 39 22. B. Mohan, H. Woo, S. Jang, S. Lee, S. Park and K. H. Park, *Solid*
40 *State Sci.*, 2013, 22, 16-20.
- 41 23. R. Wang, D. Jia and Y. Cao, *Electrochimica Acta*, 2012, 72, 101-107.
- 42 24. X. Lu, X. Wang, J. Jin, Q. Zhang and J. Chen, *Biosensors &*
43 *bioelectronics*, 2014, 62, 134-139.
- 44 25. Y. Zhang, H. Cao, W. Fei, D. Cui and N. Jia, *Sensors and Actuators*
45 *B: Chemical*, 2012, 162, 143-148.
- 46 26. G.-c. Liu, L.-m. Chen, X.-c. Duan and D.-w. Liang, *Transactions of*
47 *Nonferrous Metals Society of China*, 2008, 18, 897-903.
- 48 27. H. Zheng, X. Ma, L. Chen, Z. Lin, L. Guo, B. Qiu and G. Chen,
49 *Analytical Methods*, 2013, 5, 5005.
- 50 28. H. Nasef, V. C. Ozalp, V. Beni and C. K. O'Sullivan, *Analytical*
51 *biochemistry*, 2010, 406, 34-40.
- 52
53
54
55
56
57
58
59
60

1
2
3
4
5
6
7
8
9
10
11
12
13
14
15
16
17
18
19
20
21
22
23
24
25
26
27
28
29
30
31
32
33
34
35
36
37
38
39
40
41
42
43
44
45
46
47
48
49
50
51
52
53
54
55
56
57
58
59
60



328x140mm (96 x 96 DPI)

1
2
3 **Graphical abstract for the manuscript entitled “Shell-like Sm-doped CeO₂**
4 **nanoparticle based electrochemical DNA biosensor for breast cancer gene**
5 **sequence detection”**
6

7
8 A novel nanocomposite including chitosan, Sm-doped cerium dioxide and room
9 temperature ionic liquid was applied to sensitive detection of the breast cancer gene
10 sequence.
11
12
13
14
15
16
17
18
19
20
21
22
23
24
25
26
27
28
29
30
31
32
33
34
35
36
37
38
39
40
41
42
43
44
45
46
47
48
49
50
51
52
53
54
55
56
57
58
59
60